Supporting information

$Cu_{2-x}GeS_3$: A New Hole Transporting Material for Stable and Efficient Perovskite Solar Cell

Xin Jin,[a] Xunyong Lei,[b] Chunyan Wu,[a] Guoshun Jiang,[a] Weifeng Liu,[a] Hualing Zeng,[*,b] Tao Chen,[*,a] Changfei Zhu[*,a]

[a.] Key Laboratory of Materials for Energy Conversion, Chinese Academy of Sciences, Department of Materials Science and Engineering, University of Science and Technology of China, No. 96 Jinzhai Road, Hefei, Anhui Province, 230026 *E-mail: T. Chen. tchenmse@ustc.edu.cn, C. F. Zhu. cfzhu@ustc.edu.cn

[b.] ICQD, Hefei National Laboratory for Physical Science at the Microscale, and CAS Key Laboratory of Strongly-coupled Quantum Matter Physics, The University of Science and Technology of China, No. 96 Jinzhai Road, Hefei, Anhui Province, 230026 * E-mail: H. L. Zeng. hlzeng@ustc.edu.cn

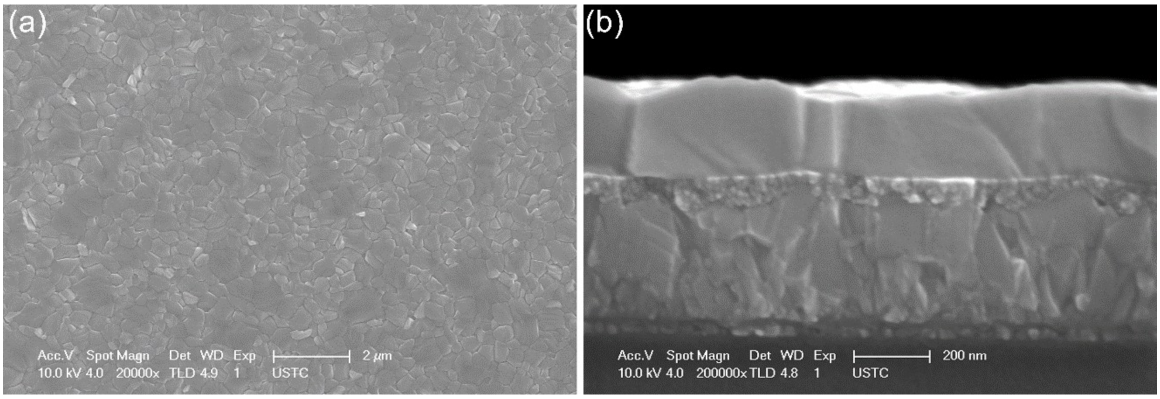

Figure S1. (a) Surface and (b) cross-sectional SEM images of $MAPbI_3$ film.

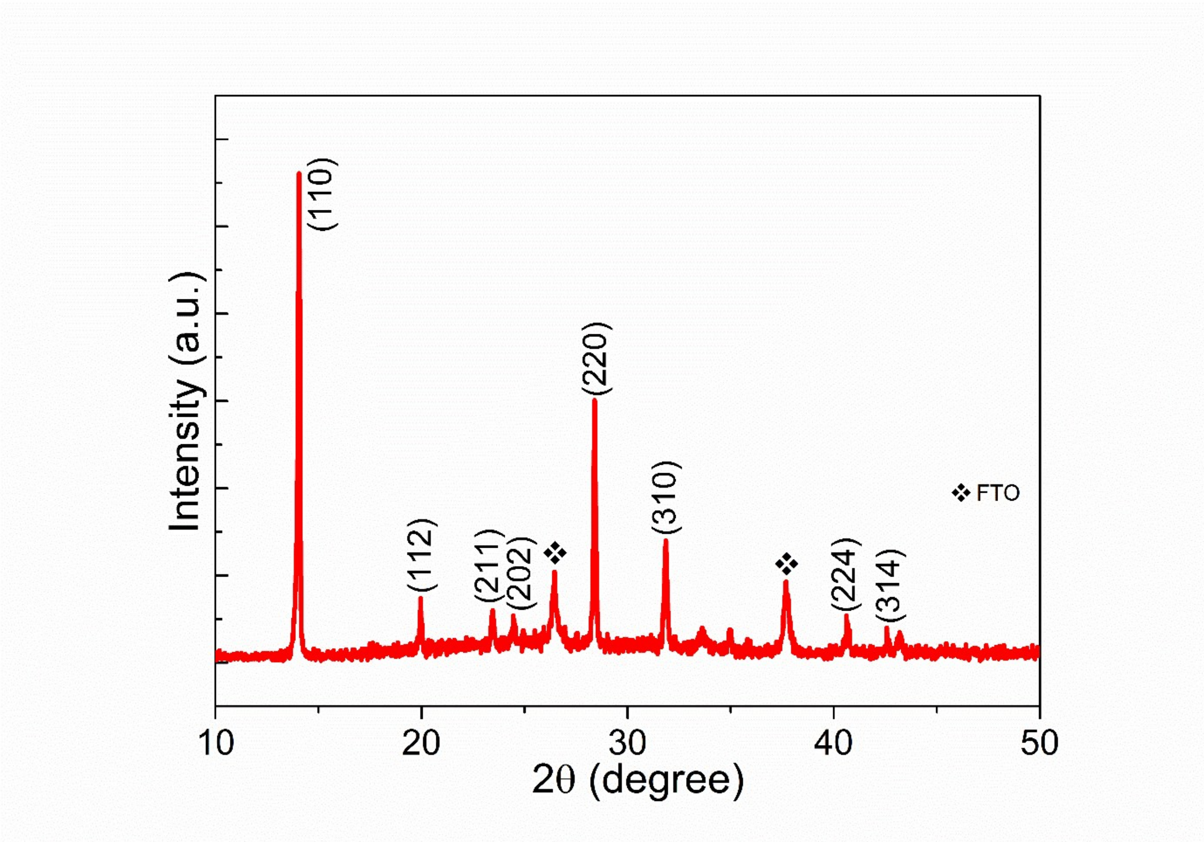

Figure S2. XRD pattern of the as-synthesized $MAPbI_3$ film, showing tetragonal phase without impurities.

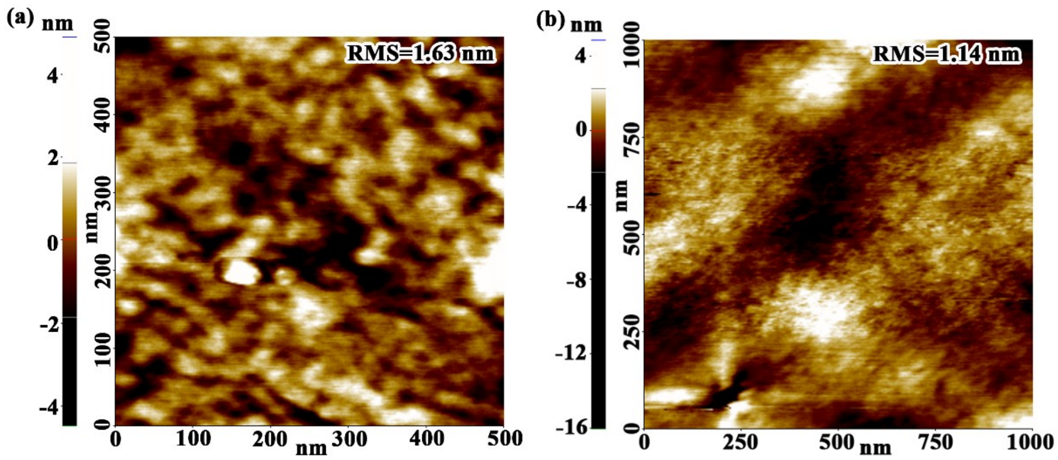

Figure S3. AFM height images of (a) CGS and (b) spiro-OMeTAD films deposited on $MAPbI_3$.

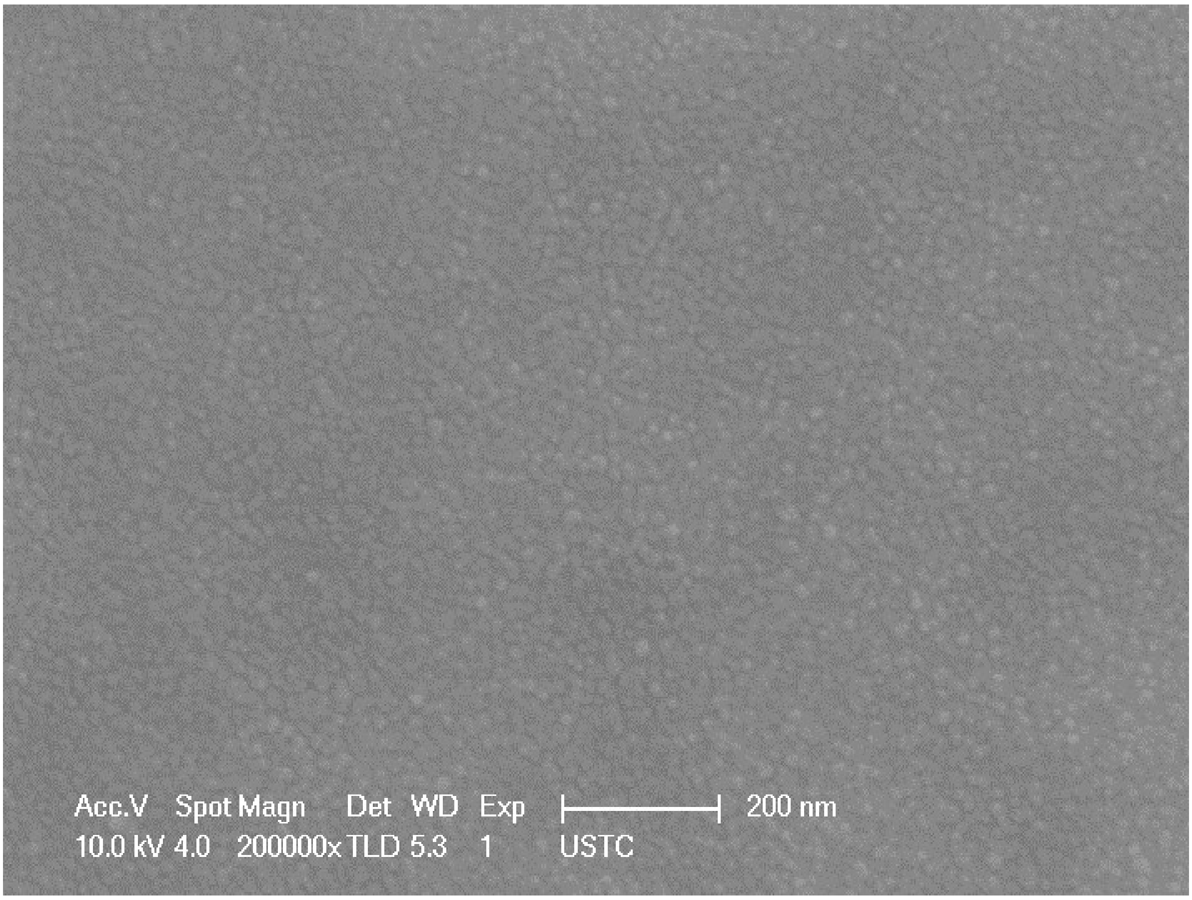

Figure S4. Surface SEM image of CGS film coated on perovskite.

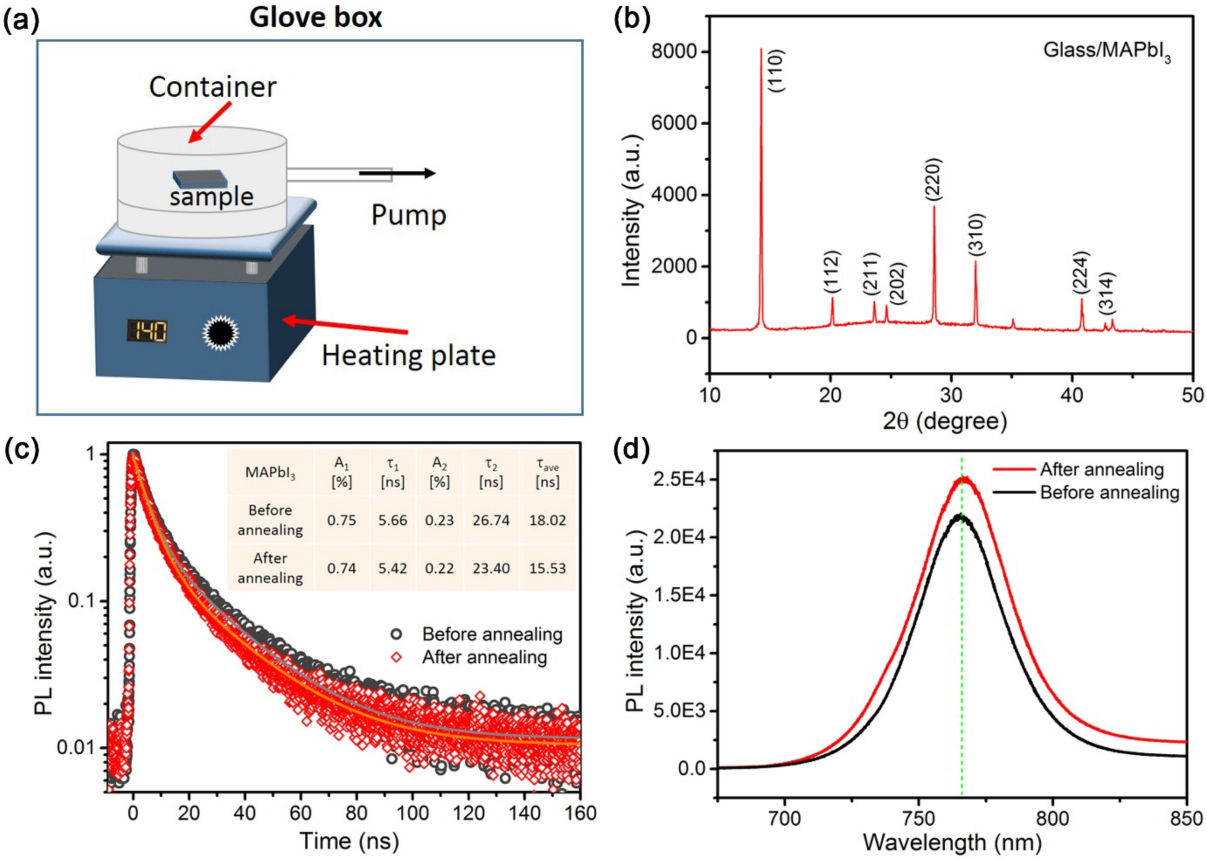

Figure S5. (a) Schematic illustration of home-made annealing equipment placed in nitrogen-filled glove box. (b) XRD pattern of bare $MAPbI_3$ film deposited on glass. (c) Time-resolved photoluminescence decay measurements and (d) steady-state photoluminescence spectra for the bare $MAPbI_3$ thin films deposited on glass before and after annealing.

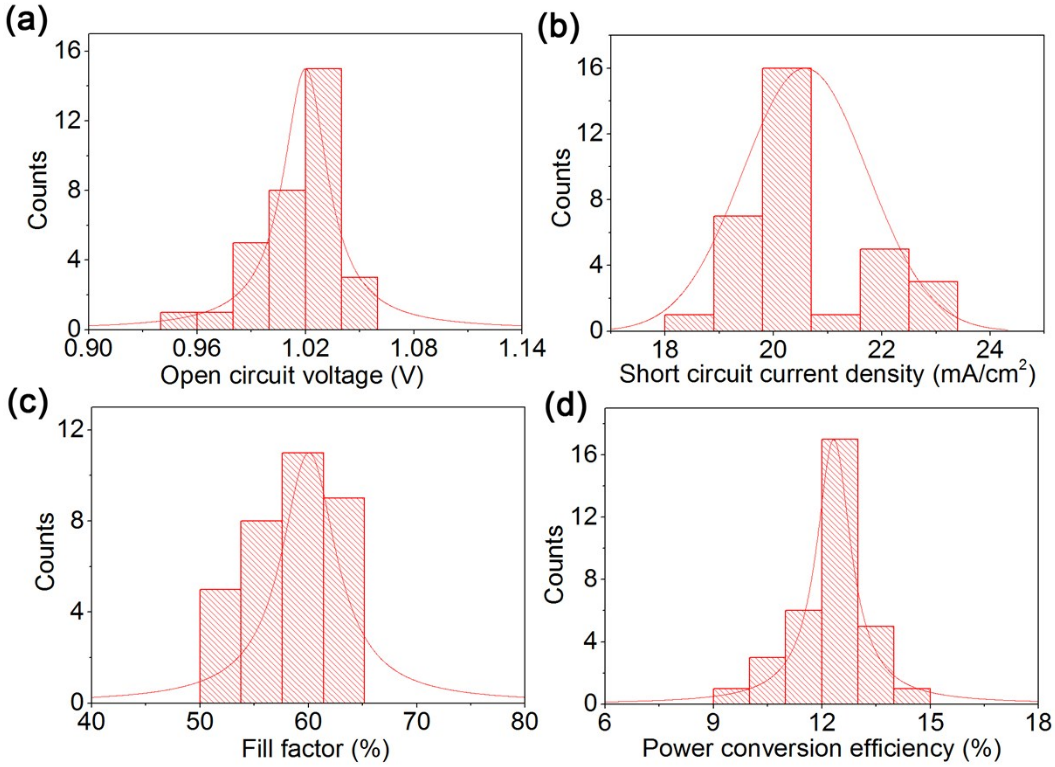

Figure S6. Histogram of solar cell parameters measured for 34 separate devices fabricated under the optimized condition for CGS hole transporting layer: 4000 rpm for 30 s, followed by annealing at ~140 °C for 5 min.

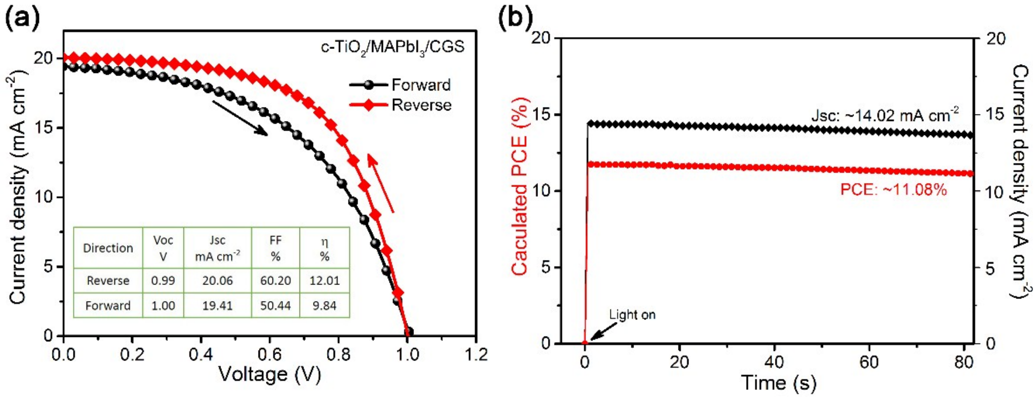

Figure S7. (a) J-V curves of CGS-based device with different scan directions. (b) Stabilized photocurrent output at 0.75 V bias and calculated power conversion efficiency.

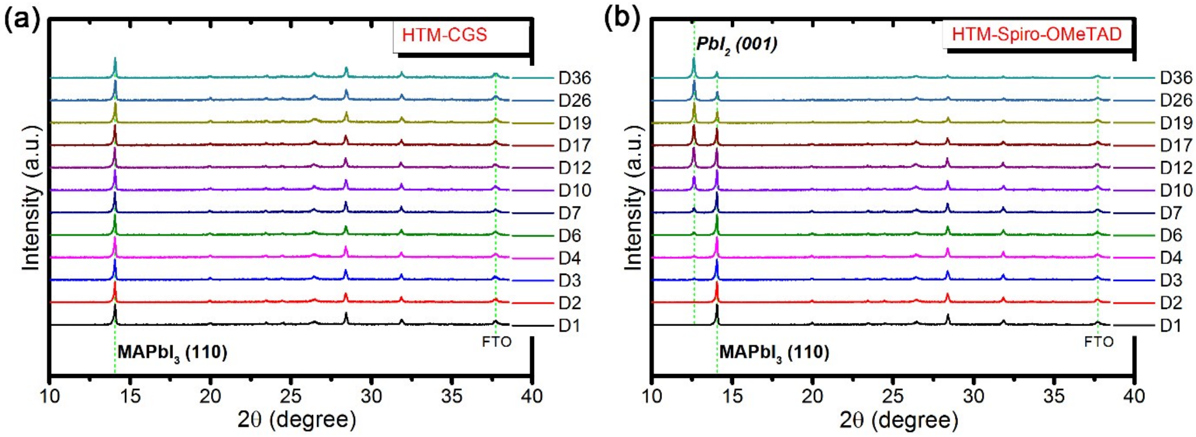

Figure S8. Diffraction patterns of $MAPbI_3$ films coated with (a) CGS and (b) spiro-OMeTAD storing under relative humidity of 50% at 25 °C in air for different durations, D1 to D36 represent storing for 1 day to 36 days.

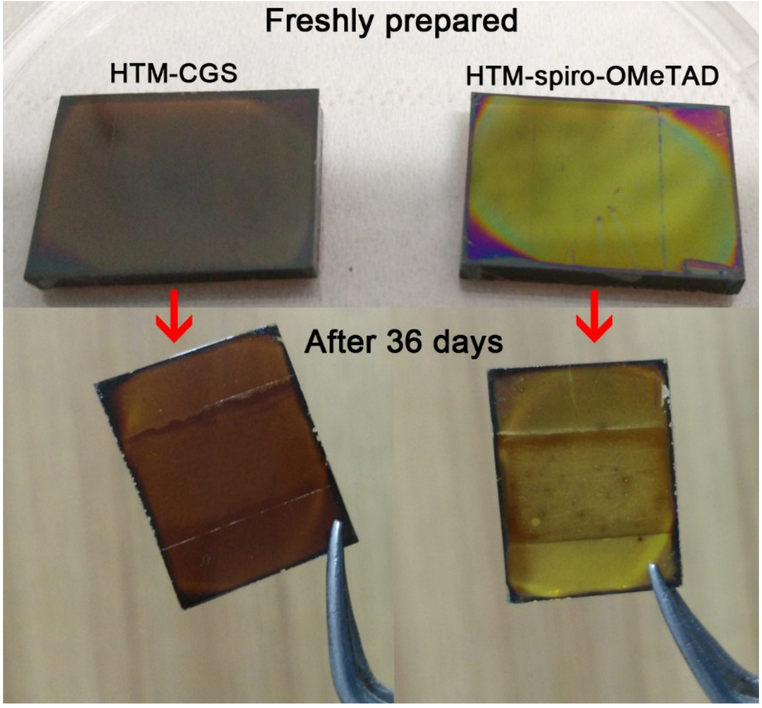

Figure S9. Digital photos illustrating the visible degradation of the perovskite layer after 36 days. The color of $MAPbI_3$ film covered with CGS remained unchanged, while the spiro-OMeTAD-based one showed rough surface with the precipitation of PbI_2.

Table S1. Fitting parameters for the time-resolved photoluminescent decay curves of glass/$MAPbI_3$, glass/$MAPbI_3$/CGS and glass/$MAPbI_3$/spiro-OMeTAD films.

Sample	A_1 [%]	τ_1 [ns]	A_2 [%]	τ_2 [ns]	τ_{ave} [ns]
Perovskite	0.75	5.66	0.23	26.74	18.02
Spiro-OMeTAD	0.75	2.25	0.13	11.76	6.79
CGS	0.76	1.56	0.14	8.26	4.86

Table S2. Photovoltaic parameters of $MAPbI_3$ perovskite solar cells based on CGS HTL with various Cu/Ge ratios.

Cu/Ge ratio	V_{OC} [V]	J_{SC} [mA/cm^2]	FF [%]	η^a [%]	R_S [$\Omega\cdot cm^2$]	R_{Sh} [$\Omega\cdot cm^2$]
1.57	1.03	16.83	46.8	8.15	26.49	698.89
1.66	1.08	16.63	58.9	10.56	14.83	1349.05
1.72	1.04	15.77	47.1	7.74	22.09	456.95
1.80	1.06	14.21	46.5	6.97	29.63	501.37
1.90	1.08	11.15	28.7	3.45	88.11	141.47
3.37	0.90	0.00	24.9	0.00	1156990.48	928303.11

a. In this case, we are trying to find the optimum Cu/Ge ratio of the CGS for hole transporting in the perovskite solar cell, the annealing temperature and duration of CGS films are not optimized. As a result, when the Cu/Ge ratio is 1.66 in CGS nanoparticles, the device generates the highest power conversion efficiency. The following optimizations on the annealing temperature and duration are thus based on the CGS nanoparticle with this elemental ratio.

Table S3. Thickness dependence of device performance using Cu_2GeS_3 as HTL with the structure of TiO_2/$MAPbI_3$/CGS/Au.

CGS thickness^a	V_{OC} [V]	J_{SC} [mA/cm^2]	FF [%]	η [%]	R_S [$\Omega\cdot cm^2$]	R_{Sh} [$\Omega\cdot cm^2$]
390 nm	1.09	13.47	33.37	4.91	59.50	261.71
250 nm	1.08	15.49	48.64	8.17	28.07	1499.98
150 nm	1.09	15.92	50.21	8.69	26.61	1378.58
120 nm	1.09	16.52	57.90	10.47	16.42	3707.47
100 nm	1.09	16.07	54.04	9.13	22.31	1770.71
80 nm	1.07	13.96	53.98	8.09	29.82	357.42
60 nm	1.06	11.14	53.85	6.34	38.10	301.40

a. In experiment, we adopt an easy method to control the thickness of CGS by spin speed. When the spin speed increased from 1000 rpm to 7000 rpm with a step of 1000 rpm, the thickness of CGS decreased from 390 nm to 60 nm, respectively. The measurement results show that 120-nm-thick $Cu_{2-x}GeS_3$ (4000 rpm, 30 s) give the highest PCE of 10.47% with a small R_s and a large R_{sh}.

Table S4. Device parameters for perovskite solar cells using CGS hole transporting layer with post annealing at different temperatures for 10 min.

Annealing temperature	V_{OC} [V]	J_{SC} [mA/cm^2]	FF [%]	η [%]	R_S [Ω·cm^2]	R_{Sh} [Ω·cm^2]
60 ^{o}C	1.01	16.58	34.22	5.75	55.35	222.22
80 ^{o}C	1.02	17.34	42.98	7.58	30.49	385.74
100 ^{o}C	1.04	17.79	51.53	9.49	17.47	828.84
120 ^{o}C	1.03	18.32	59.27	11.21	13.27	2024.49
140 ^{o}C	1.03	17.84	63.20	11.60	11.48	1774.99

Table S5. Device parameters for perovskite solar cells using CGS hole transporting layer annealed under 140°C for different times.

Annealing time	V_{OC} [V]	J_{SC} [mA/cm^2]	FF [%]	η [%]	R_S [Ω·cm^2]	R_{Sh} [Ω·cm^2]
0 min	1.08	16.82	45.12	8.21	28.32	567.45
5 min	1.06	18.55	63.80	12.56	11.69	2241.98
10 min	1.03	19.28	55.10	10.93	16.22	1040.05
15 min	0.99	17.77	38.40	6.76	36.23	355.62

With the above optimizations (Table S2-S5), the final fabrication condition for the CGS HTL is CGS nanoparticles with Cu/Ge ratio of 1.66, spinning coating at 4000 rpm for 30 s, post annealing at 140 °C for 5 min. The distribution of the device fabricated at this optimized condition is shown in Figure S6.